Interface reconstruction and dislocation networks for a metal/alumina interface: an atomistic approach

2008 J. Phys.: Condens. Matter 20 135005

(http://iopscience.iop.org/0953-8984/20/13/135005)

J. Phys.: Condens. Matter **20** (2008) 135005 (7pp) doi:10.1088/0953-8984/20/13/135005

Interface reconstruction and dislocation networks for a metal/alumina interface: an atomistic approach

Y Long[1,2] **and N X Chen**[1,3]

[1] Department of Physics, Tsinghua University, Beijing 100084, People's Republic of China
[2] Center for Advanced Study, Tsinghua University, Beijing 100084, People's Republic of China
[3] Institute for Applied Physics, University of Science and Technology, Beijing 100083, People's Republic of China

E-mail: longyao@tsinghua.org.cn

Received 26 November 2007, in final form 22 January 2008
Published 7 March 2008
Online at stacks.iop.org/JPhysCM/20/135005

Abstract

Misfit dislocation is an important component of the semi-coherent interface. Usually, it forms a dislocation network as the strain concentration area on an interface and makes the other part coherent. This is the regular case, but there are also some exceptions. In this work, we show that the Ni/$(Al_2O_3)_{Al}$ interface has a reconstruction at the first monolayer of the metal side, which works as a transition layer between Ni and Al_2O_3 lattices. Under these conditions, the misfit dislocation cannot be confirmed by drawing a Burgers circuit because the interface is incoherent. However, due to the lattice misfit, there are areas of strain concentration and areas without strain distributed on the interface plane. So, for describing this strain distribution, we again use the concept of a dislocation network but redefine it as the separate line between these two parts. As a result, we find that the dislocation network appears when the metal part is thicker than 12.4 Å, and it shrinks as the metal film grows, resulting in an ultimate structure with a mesh size of 28.1 Å.

(Some figures in this article are in colour only in the electronic version)

1. Introduction

The metal/oxide interface is a hot problem in current science and technology, and has many applications in catalysts, composites, metal-ceramic sensors, etc [1–4], so it has attracted many theoretical studies. Among the various interface systems, metal/MgO and metal/Al_2O_3 ones have attracted much attention in terms of their electronic structure, adhesion, wetting ability, misfit dislocation, etc [5–9]. So in our previous works we have made many efforts to study the misfit dislocation in metal/MgO systems [10, 11], and have shown a regular tetragonal dislocation network for them. However, the case is quite simple for metal/MgO in that it just contains two groups of perpendicular dislocation lines (DLs). But it becomes complex for metal/Al_2O_3 because a dislocation loop or partial dislocation appears in this case, accompanied by a hexagonal or trigonal dislocation network [5, 12]. We now turn to this complex case and try to get a theoretical description of the dislocation network in hexagonal or trigonal structures.

In this work, we are going to study the Ni/Al_2O_3 interface, mainly focusing on the case of an Al terminated interface (or briefly, Ni/$(Al_2O_3)_{Al}$). There are two reasons for us to choose an Al terminated interface as the target system rather than the O terminated one. First is that we have driven the pair potentials across a Ni/Al_2O_3 interface in our previous work [13], and shown their transferability on a series of metastable structures for Ni/$(Al_2O_3)_{Al}$. Second, Ni/$(Al_2O_3)_{Al}$ is also the energy preferred interface. It has an adhesive energy of 1.3–1.9 eV due to some *ab initio* works, while the one for an O terminated interface is 6.3–7.1 eV [13–15]. Considering the experimental results between 1.1 and 1.2 eV [16, 17], the Al terminated interface is preferred.

There are two main purposes for this work. First is to determine the interface structure and second is to evaluate the dislocation network. It is very interesting that the Ni/$(Al_2O_3)_{Al}$ interface has a reconstruction at the first monolayer (ML) of the metal side (see the work below), so its misfit dislocation is different from the regular case defined by a Burgers circuit. Now, the dislocation network is redefined as the separate line between the area of strain concentration and the area with no strain on the interface, and so we can proceed with further studies on it.

The following work consists of four parts. First, in section 2, we present the interatomic potentials for the Ni/Al_2O_3 interface of both the metal–oxide and metal–metal cases. They are *ab initio* based pair potentials obtained in our previous work, and are now used for some advanced studies. In section 3, we study the relaxed structure of the Ni/$(Al_2O_3)_{Al}$ interface. An interface reconstruction is obtained at the first ML of the metal side, and works as a translation layer between Ni and Al_2O_3 lattices. Next, in section 4, we go into the main part of this paper and demonstrate a theoretical evaluation of the dislocation network. As a result, we find that the dislocation network appears in the Ni/$(Al_2O_3)_{Al}$ interface when the metal side is thick enough, shrinks as the metal film grows, and tends to an ultimate structure. Finally, section 5 is the conclusion.

2. Interatomic potentials

Usually, the atomistic simulation for a target system is based on some interatomic potentials. The validity and practicability of these potentials is the first important issue. For the Ni/Al_2O_3 interface considered in this work, we use the pair potentials extracted from *ab initio* cohesive and adhesive energies by a Chen–Möbius inversion method [13, 18].

In detail, the Ni/Al_2O_3 interface contains three kinds of potentials: the metal–oxide, metal–metal, and oxide–oxide interactions. The first of these occurs across the interface, and the latter two in the inner bulk materials.

The metal–oxide potentials have been obtained in our previous work [13]. We have shown that they prefer an Al terminated interface, but should avoid an O terminated interface. This is why we chose to study Ni/$(Al_2O_3)_{Al}$ in this work but not Ni/$(Al_2O_3)_O$.

Regarding the oxide side, Al_2O_3 has a more complex structure and charge distribution than metal, and this gives us some difficulties in obtaining its interatomic potentials. So before achieving the final solution of Al_2O_3, we use the metal–oxide and metal–metal potentials to proceed with a basic study on the Ni/Al_2O_3 interface. At this condition, the Al_2O_3 lattices are fixed, and so the oxide–oxide potentials are not necessary. This is a primary approximation of the metal/oxide interface system but sometimes reasonable. Because Al_2O_3 as an ionic crystal is more rigid than metal, so the interface relaxation is mainly distributed in the metal side. Furthermore, fixing Al_2O_3 lattices can greatly reduce the free variables in the energy minimization calculation, and so we can study the interface on a large scale.

Table 1. Potential parameters for Φ_{Ni-Ni}.

	a_i (eV)	b_i (Å^{-1})	c_i (Å)
1	−5.85	2.29	1.83
2	−11.71	0.94	0.17
3	1.17	0.85	0.86
$D_0 = 52.60$ eV			
$R_0 = 1.00$ Å			
$y = 2.22$			

Table 2. The lattice constant (a) and elastic constants (C_{11}, C_{12}, and C_{44}) for bulk Ni.

	a (Å)	C_{11} (GPa)	C_{12} (GPa)	C_{44} (GPa)
This work	3.50	263.2	183.5	183.5
Expt. [19]	3.52	248.1	154.9	124.2

For the metal side, the metal–metal potential Φ_{Ni-Ni} is extracted from *ab initio* cohesive energies by the Chen–Möbius inversion method [18]. Now, for an improved description of the elastic constants, we do not use the Morse potential as appears in our previous work [11], but recalculate it in a more precise way, resulting in a Rahman–Stillinger–Lemberg potential (1), as shown in table 1.

$$\Phi = D_0 e^{y(1-\frac{r}{R_0})} + \frac{a_1}{1+e^{b_1(r-c_1)}} + \frac{a_2}{1+e^{b_2(r-c_2)}} + \frac{a_3}{1+e^{b_3(r-c_3)}}. \quad (1)$$

As a basic check, table 2 shows the lattice and elastic constants obtained by the above potential, including both the theoretical and experimental values. Among the four parameters, a, C_{11}, and C_{12} are in good agreement with experiments, while C_{44} is not so good in this comparison. The poor agreement for C_{44} is related to the Cauchy relation $C_{12} = C_{44}$ led by the pair potential approach for cubic metals. Fortunately, in this work we consider the edge dislocation in the metal side where the lattice distortion is limited in tensile strain, without any transformation of the crystal angles. So C_{11} and C_{12} play a more important role than C_{44} in describing the elastic field around DLs, and this pair potential approach is sometimes reasonable.

In summary, we use a pair potential model in this work. It seems a very simple approximation to the interface system not to take the many body effect and charge transfer into account but, due to the above discussion and checking, this pairwise approach is also a reasonable description of the metal/oxide interface, and has already shown its applications in metal/MgO interfaces [10, 11]. So we use it again here to treat the metal/Al_2O_3 interface, trying to get a theoretical understanding of the interface reconstruction and dislocation network.

3. Interface structure

In this work, we study the Ni/$(Al_2O_3)_{Al}$ interface with an orientation relationship of Ni(111) ∥ Al_2O_3(0001), and mainly pay attention to the interface structure and misfit dislocation. Regarding the geometric property of this interface, the lattice constant is $a_{Ni} = 3.52$ Å for Ni and $a_{Al_2O_3} = 4.76$ Å for Al_2O_3,

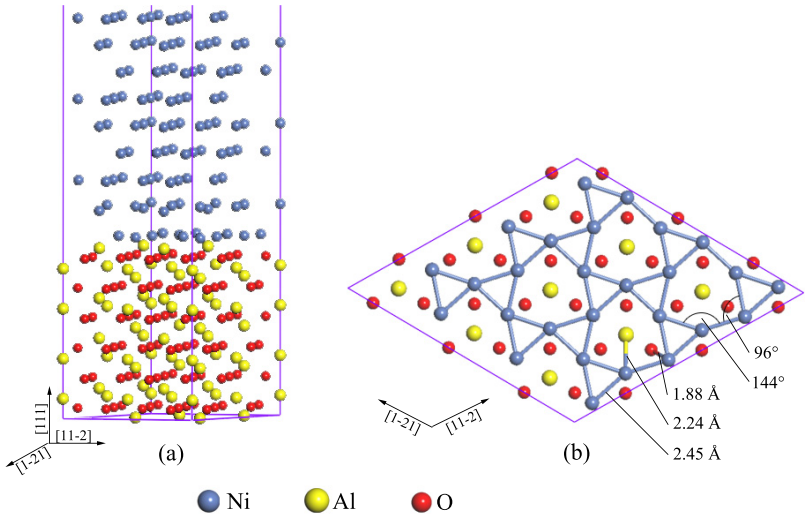

Figure 1. The relaxed interface structure of Ni/$(Al_2O_3)_{Al}$: (a) side view, (b) top view. Note that in (b), we just present the first ML of the Ni side and the first two MLs of the Al_2O_3 side for a detailed description.

so it has a 9.3% misfit between the two parts, obtained by the formula:

$$\frac{a_{Al_2O_3} - \sqrt{\frac{3}{2}}a_{Ni}}{a_{Al_2O_3}}. \qquad (2)$$

The first important issue about the interface is its structure, which is determined as in the lowest energy state. In this section, we use an energy minimization method to treat this problem, paying attention to the possible reconstruction on the interface.

Cerius[2] software is used for the energy minimization calculation [20], accompanied with the periodic boundary condition. For the interface model, the Al_2O_3 part is 12 Å thick and the Ni part is 10–100 Å thick. Note that Al_2O_3 lattices are fixed in this calculation, so 12 Å is enough to support the metal lattices and misfit dislocation.

Some *ab initio* works [14, 15] have shown that the lowest energy structure of the Ni/$(Al_2O_3)_{Al}$ interface is of metal on an O site. This is the energy preferred site for an Al terminated interface and is also supported by our pair potentials [13]. Now, the interface structure is calculated again by the energy minimization method [20], resulting in a totally relaxed model, as shown in figure 1.

From the figure, we see that Ni/$(Al_2O_3)_{Al}$ is reconstructed at the first ML of the metal side. Its trigonal structure is rearranged as a combination of a regular triangle and an irregular hexagon, as shown in figure 1(b). For a quantitative description of this reconstruction, the Ni–Ni distance is 2.45 Å, Ni–O distance is 1.88 Å, Ni–Al distance is 2.24 Å, and the hexagon angles are 96° and 144°.

As a result, the reconstructed Ni ML works as a translation layer between Ni and Al_2O_3 sides, and makes the interface incoherent. At this condition, the misfit dislocation cannot be confirmed by a Burgers circuit, but needs a new definition. Note that the misfit strain is not equally distributed on the whole interface plane, but has an area of strain concentration and an area without strain. So we define DL as the separate line between these two parts, and use it for advanced studies.

This kind of reconstruction for an Ni/$(Al_2O_3)_{Al}$ interface has been reported in Wang's *ab initio* work [21], which also shows a combination of regular triangle and irregular hexagon structures for the first ML of the Ni side. Considering this agreement, our work shows that the pair potential approach can give a good description of the interface structure and reconstruction, and supports the need for our advanced study on mismatch interfaces.

4. Dislocation networks

We are now going to deal with the main part of this work: the atomistic simulation of a dislocation network in an Ni/$(Al_2O_3)_{Al}$ interface. In this section, we show the method of obtaining a misfit dislocation and then calculate the DL position as well as the dislocation structure, resulting in a theoretical evaluation of the dislocation network.

4.1. Methodology

Usually, a concrete interface contains a dislocation network as the strain concentration centre, and makes the other part coherent. This dislocation network has several kinds of geometric structures at different interface systems. For example, for a metal/MgO interface, it is in a tetragonal structure, constructed by two groups of perpendicular DLs. This is a very simple case for which, due to the orthogonality, we can use a cross-section model instead of the whole interface to study the misfit dislocation, as shown in our previous works [10, 11]. But for a metal/Al_2O_3 interface, the case becomes complex, since the dislocation network is in a hexagonal or trigonal structure, and usually accompanied with dislocation loops or partial dislocations [5, 12]. Under these conditions we cannot just use a cross-section model, but need to consider the whole interface.

As the Ni/Al_2O_3 interface has a positive misfit of 9.3%, we use a $(n + 1 \times n + 1)$:$(n \times n)$ interface model to obtain the

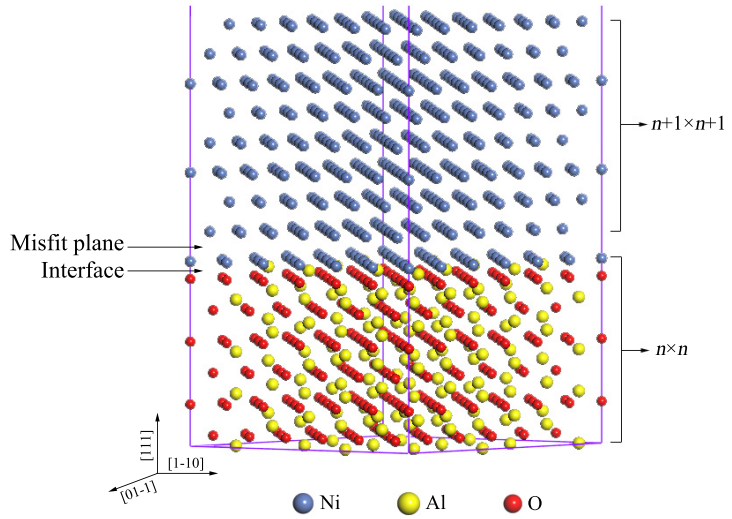

Figure 2. The $(n + 1 \times n + 1)$:$(n \times n)$ interface model, for which $n = 6$ and the mismatch plane is at the second ML of the metal side.

misfit dislocation, as shown in figure 2. This is the initial model waiting for energy minimization, and the dislocation is placed in the metal side because Al_2O_3 is more rigid than metal.

Furthermore, for an energetic evaluation of the dislocation structure and network, we need to extract the dislocation energy (E_{dis}) from the energy minimization result. Generally, the total energy (E_{total}) of a certain interface system contains several parts, including the contributions of lattice, surface, interface, and misfit dislocation. In particular, in this work, the interface model is of a metal film supported on an oxide surface, as shown in figure 2. So except for the interface, the metal part also has an upper surface in contact with a vacuum, with the surface area equal to the interface area (S). In addition, as we have fixed the oxide part in the energy minimization, its surface and lattice energies are not considered. As a result, the 'energy extract formula' is

$$E_{dis} = E_{total} - n_{Ni}\varepsilon_{Ni} - S(\sigma_{Ni} + \sigma_{Ni/Al_2O_3}) \qquad (3)$$

where ε_{Ni} is the lattice energy, σ_{Ni} is the surface energy, σ_{Ni/Al_2O_3} is the interface energy, and n_{Ni} is the number of metal atoms. About these parameters, ε_{Ni}, σ_{Ni}, and σ_{Ni/Al_2O_3} are obtained by calculating some ideal models, with the result of $\varepsilon_{Ni} = -5.18$ eV, $\sigma_{Ni} = 0.40$ eV Å^{-2}, and $\sigma_{Ni/Al_2O_3} = 0.15$ eV Å^{-2}.

This formula has already been used in our previous works to study metal/MgO interfaces [10, 11], and has shown its suitability in describing the energetic properties of misfit dislocations. Therefore, we use it again in this work to treat the metal/Al_2O_3 interface.

4.2. Dislocation position

A basic parameter of a misfit dislocation in a metal/oxide interface is the position of the DL. Usually, it is in the first ML of the metal side for metal/MgO interfaces [10, 11]. But for the case of Ni/$(Al_2O_3)_{Al}$, this layer is reconstructed, so the DL may be in some other positions. A careful reconsideration is desired.

Generally, the DL position is related to the position (P) of the mismatch plane in the initial model. Above this plane, the cell is $n + 1 \times n + 1$, and below it, the cell is $n \times n$, as shown in figure 2 for the case of $P = 2$. For determining the DL position, we are going to search through $P = 1$–9, by using the energy minimization program [20] and 'energy extract formula' (3).

Figure 3(a) shows the resultant dislocation energies for $P = 1$–9, where we consider the average energy per interface area $\frac{E_{dis}}{S}$. As a result, the energy preferred position is $P = 2$.

For a discussion, we present the relaxed interface structures of $P = 1$–3 in figures 3(b)–(d). Factually, the $P = 1$ case is a totally distorted structure. This is because the Ni/$(Al_2O_3)_{Al}$ interface has a reconstruction at the first ML of the metal side, which is destroyed by putting DL in this position. Comparatively, the $P = 2$ case has an orderly lattice structure in the metal side, while the $P = 3$ case is sometimes distorted at the first two Ni MLs. Among them, DL in the second ML of the metal side makes a regular interface structure, and also has the lowest dislocation energy.

4.3. Dislocation network

In this work, the first Ni ML is reconstructed as a translation layer between metal and Al_2O_3 sides, and DL is redefined as the separate line between the strain concentration area and the area with no strain on the interface. So we can show the dislocation network by plotting the Ni–Ni distance distribution of the second Ni ML, as shown in figure 4(a).

As we have mentioned in section 4.1, a misfit dislocation is introduced by a $(n + 1 \times n + 1)$:$(n \times n)$ mismatch interface. So the dislocation network makes Ni lattices compressed. As a result, the Ni–Ni distance is in a lower value for the strain concentration area (the small deep gray part (red online) part in figure 4(a)), and in a higher value for the area with no strain (the large deep gray part (blue online) part in figure 4(a)). This figure shows that the strain concentration area and the area with no strain appear

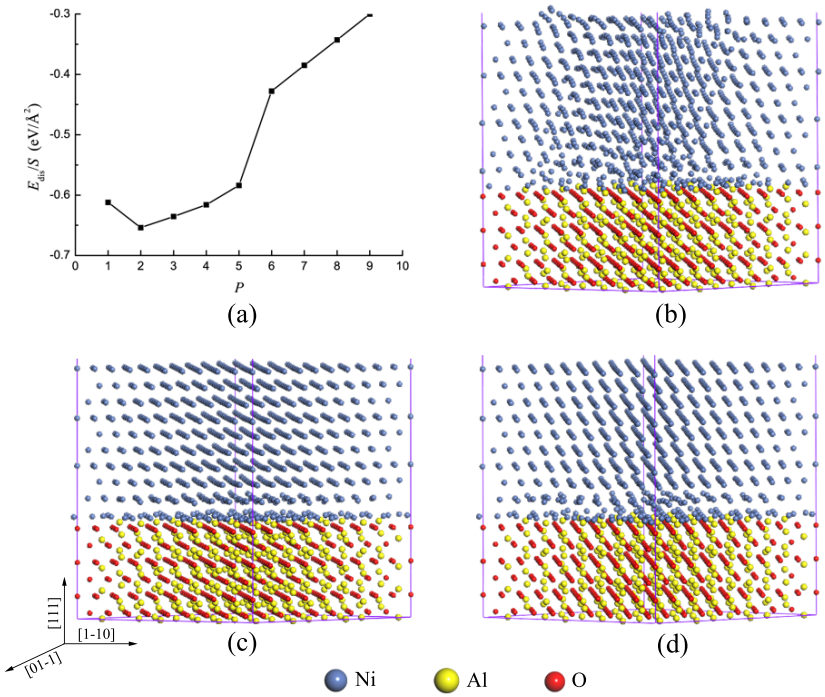

Figure 3. (a) The average dislocation energy $\frac{E_{dis}}{S}$ for $P = 1$–9, (b) the relaxed interface structure of $P = 1$, (c) $P = 2$, and (d) $P = 3$, where $n = 9$ for this test.

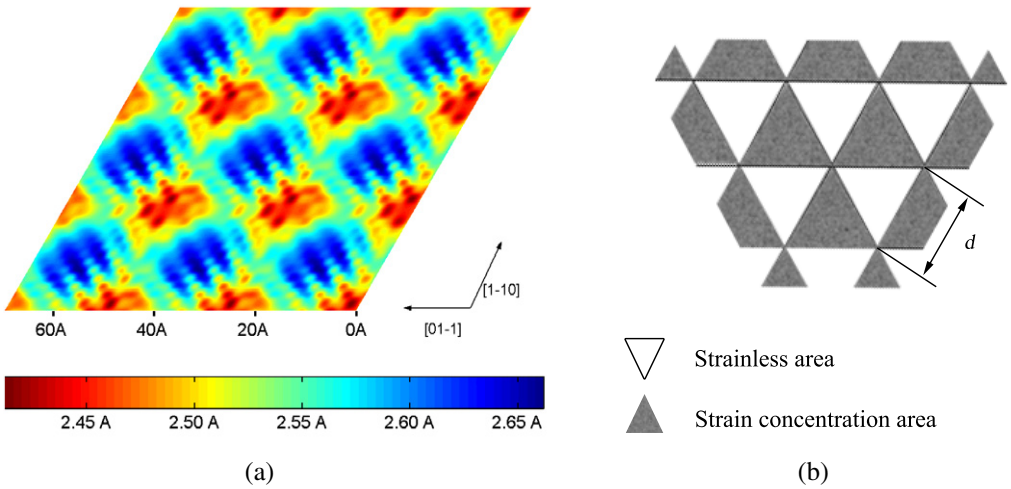

Figure 4. The dislocation network of the Ni/$(Al_2O_3)_{Al}$ interface. (a) The Ni–Ni distance distribution of the second Ni ML, in the case of $n = 9$; (b) the summarized dislocation network structure.

alternately on the interface plane, approximately resulting in a trigonal dislocation network, as shown in figure 4(b). At this condition, the DL is a partial dislocation along the $[1\bar{1}0]$ direction, with Burgers vector $b = \frac{1}{6}[11\bar{2}]$, and the mesh size d for dislocation network is proportional to n, with $\frac{d}{n} = 2.75$ Å, where 2.75 Å is the O–O distance. By the way, concerning the dislocation network in a hexagonal interface, Ernst [12] has shown two representative cases, in hexagonal and trigonal structures respectively. Among them, the former contains dislocation loops and the latter contains partial dislocations. Our contribution is to confirm the trigonal case for an Ni/$(Al_2O_3)_{Al}$ interface on the atomic scale.

For a discussion of the mesh size d, $\frac{1}{d}$ is proportional to the misfit across the interface, and so is related to the relaxation energy brought by a misfit dislocation. For an Ni/$(Al_2O_3)_{Al}$ interface, the dislocation energy contains four parts. First is the relaxation energy, which is related to $\frac{1}{d}$ and proportional to metal volume V. The second to fourth are dislocation network energies, including the contributions of the strain concentration area (σ), dislocation line (ε), and intersection point between DLs (c). As a result, we get the 'dislocation energy formula':

$$E_{dis} = cN + \varepsilon L + \sigma\frac{S}{2} + K_1 V\delta + K_2 V\delta^2 + K_3 V\delta^3 + K_4 V\delta^4 \quad (4)$$

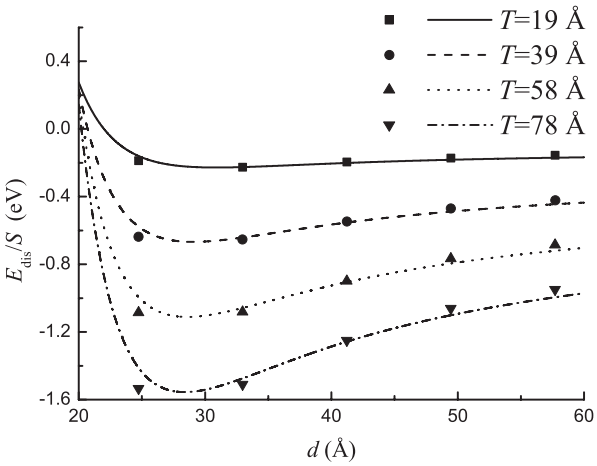

Figure 5. The fitting results of E_{dis} versus d curves by (4), for which $T = 19$, 39, 58, and 78 Å. The scatter symbols denote the original E_{dis} data and the lines denote fitted curves.

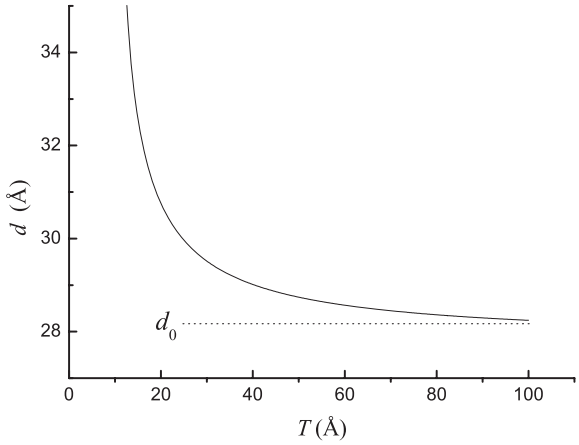

Figure 6. The energy preferred size d as a function of T.

where $K_1V\delta + K_2V\delta^2 + K_3V\delta^3 + K_4V\delta^4$ is the relaxation energy, S is the interface area, L is the total length of DLs, N is the number of intersection points, and $\delta = \frac{a_{Ni}}{d}$ is a nondimensional parameter. In (4), the relaxation energy is a fourth-order Taylor expansion, with the zeroth-order term equals to zero. This is because relaxation energy is brought by misfit dislocation. If there is no dislocation on the interface (or $\delta \to 0$), it reduces to zero.

Equation (4) is used to evaluate E_{dis} from d and V directly. By using this formula, we can get the dislocation energy just by a simple calculation, and study the Ni/$(Al_2O_3)_{Al}$ interface on a large scale. Turning back to the constitution of (4), there are seven undetermined parameters c, ε, σ, K_1, K_2, K_3, and K_4. For evaluating them, we calculate a series of sample models by the energy minimization method [20] and the 'energy extract formula' (3), resulting in a list of E_{dis} at different combinations of d and T, as shown in figure 5, where T denotes the thickness of the metal part. For these interface models, n is from 9 to 21 and T is chosen to be 19, 39, 58, and 78 Å. As a result, the parameters for (4) are fitted by using a least squares method [22], and so we can get $c = -3.499$ eV, $\varepsilon = 1.973$ eV Å^{-1}, $\sigma = -0.025$ eV Å^{-2}, $K_1 = -0.455$ eV Å^{-3}, $K_2 = 7.042$ eV Å^{-3}, $K_3 = -70.764$ eV Å^{-3} and $K_4 = 254.569$ eV Å^{-3}.

For some advanced studies of dislocation networks, we consider the average dislocation energy $\frac{E_{dis}}{S}$ again. The energy preferred size d is picked from the minimum point of the $\frac{E_{dis}}{S}$ versus d curve. And so we can evaluate d as a function of the thickness T of the metal side.

In fact, when T is small, there is no minimum point in the $\frac{E_{dis}}{S}$ versus d curve. This means that the dislocation network is not energy preferred at this case. For the Ni/$(Al_2O_3)_{Al}$ interface, this separate line is 12.4 Å. So the appearance of a dislocation network requires the metal side to be thicker than 12.4 Å.

Figure 6 shows the resultant mesh size d as a function of T. It demonstrates that d decreases with the metal side thickness and tends to an ultimate value $d_0 = 28.1$ Å. As a result, we get the evolution of the dislocation network in the Ni/$(Al_2O_3)_{Al}$ interface. It appears that when T is greater than 12.4 Å, d shrinks as T increases, and results in an ultimate size of $d_0 = 28.1$ Å.

Also, the ultimate size can be calculated from the lattice constants a_{Ni} and $a_{Al_2O_3}$ directly, as shown in (5). By using this formula, d_0 is determined as 26.8 Å, which is in good agreement with the previous value. It shows that our method is self-consistent.

$$d_0 = \frac{a_{Al_2O_3}a_{Ni}}{\sqrt{2}a_{Al_2O_3} - \sqrt{3}a_{Ni}}. \tag{5}$$

5. Conclusion

In this work, we have used a combination of atomistic simulation and phenomenological approach to study the misfit dislocation in an Ni/$(Al_2O_3)_{Al}$ interface, and have obtained some interesting results.

First, an interface reconstruction is found at the first ML of the metal side, which changes from a trigonal structure to a combination of regular triangle and irregular hexagon. In this case, the Ni–Ni distance is 2.45 Å, the Ni–O distance is 1.88 Å, the Ni–Al distance is 2.24 Å, and the hexagon angles are 96° and 144°.

Due to this reconstruction, the misfit dislocation is placed in the second ML of the metal side for a low energy position. As a result, we get a trigonal dislocation network constructed by partial DLs, with a strain concentration area and an area without strain appearing alternately on the interface plane. Also, the DL is along the $[1\bar{1}0]$ direction, with Burgers vector $b = \frac{1}{6}[11\bar{2}]$.

Finally, the dislocation network is evaluated as a function of the metal side thickness T. When T is smaller than 12.4 Å, no dislocation appears. As T increases, the dislocation network shrinks, and results in an ultimate size $d_0 = 28.1$ Å.

Acknowledgments

This work is supported by the Nature Science Foundation of China (NSFC), No. 50531050, and the 973 project, No. 2006CB605100.

References

[1] Sanchez A, Abbet S, Heiz U, Schneider W D, Häkkinen H, Barnett R N and Landman U 1999 When gold is not noble: nanoscale gold catalysts *J. Phys. Chem.* A **103** 9573

[2] Fecht H J 1997 EPS Industrial workshop: towards applications of nano- and quasi-crystalline materials *Europhys. News* **28** 89

[3] Padture N P, Gell M and Jordan E H 2002 Thermal barrier coatings for gas-turbine engine applications *Science* **296** 280

[4] Evans A G, Hutchinson J W and Wei Y 1999 Interface adhesion: effects of plasticity and segregation *Acta Mater.* **47** 4093

[5] Dmitriev S V, Yoshikawa N and Kagawa Y 2004 Misfit accommodation at the Cu(111)/α-Al_2O_3(0001) interface studied by atomistic simulation *Comput. Mater. Sci.* **29** 95

[6] Shi S Q, Tanaka S and Kohyama M 2007 First-principles study of the tensile strength and failure of α-Al_2O_3(0001)/Ni(111) interfaces *Phys. Rev.* B **76** 075431

[7] Goniakowski J 1999 Transition metals on the MgO(100) surface: evolution of adsorption characteristics along the 4d series *Phys. Rev.* B **59** 11047

[8] Renaud G, Guénard P and Barbier A 1998 Misfit dislocation network at the Ag/MgO(001) interface: a grazing-incidence x-ray-scattering study *Phys. Rev.* B **58** 7310

[9] Renaud G and Barbier A 1999 Structure and morphology of the Pd/MgO(001) interface during its formation *Appl. Surf. Sci.* **142** 14

[10] Long Y, Chen N X and Wang H Y 2005 Theoretical investigations of misfit dislocation in Pd/MgO(001)interface *J. Phys.: Condens. Matter* **17** 6149

[11] Long Y and Chen N X 2007 Atomistic simulation of misfit dislocation in metal/oxide interfaces *Comput. Mater. Sci.* at press (doi:10.1016/j.commatsci.2007.08.007)

[12] Ernst F 1995 Metal–oxide interfaces *Mater. Sci. Eng.* R **14** 97

[13] Long Y and Chen N X 2007 Pair potential approach for metal/Al_2O_3 interface *J. Phys.: Condens. Matter* **19** 196216

[14] Zhang W, Smith J R and Evans A G 2002 The connection between *ab initio* calculations and interface adhesion measurements on metal/oxide systems: Ni/Al_2O_3 and Cu/Al_2O_3 *Acta Mater.* **50** 3803

[15] Shi S Q, Tanaka S and Kohyama M 2006 First-principles study on the adhesion nature of the α-Al_2O_3(0001)/Ni(111) interface *Modelling Simul. Mater. Sci. Eng.* **14** S21

[16] Chatain D, Coudurier L and Eustathopoulos N 1988 Wetting and interfacial bonding in ionocovalent oxide–liquid metal systems *Rev. Phys. Appl.* **23** 1055

[17] Saiz E, Cannon R M and Tomsia A P 1999 Energetics and atomic transport at liquid metal/Al_2O_3 interfaces *Acta Mater.* **47** 4209

[18] Chen N X, Chen Z D, Shen Y N, Liu S J and Li M 1994 3D inverse lattice problems and Mobius-inversion *Phys. Lett.* A **184** 347

[19] Levy M, Bass H E and Stern R R (ed) *Handbook of Elastic Properties of Solids, Liquids and Gases* vol 2 (New York: Academic)

[20] Accelrys Inc. *Cerius*^{2} *4.0* 1999 Forcefield Engines

[21] Wang X G, Smith J R and Evans A G 2006 Phase diagram for the Ni/Al_2O_3 interface and ralationships to adhesion *Phys. Rev.* B **74** 081403(R)

[22] Mansfield Merriman 2001 *A Text-Book on the Method of Least Squares* Elibron Classics (Boston: Adamant Media Corp.)